Controlled Purification of Single-Walled Carbon Nanotube Films by Use of Selective Oxidation and Near-IR Spectroscopy

Rahul Sen, Shawna M. Rickard, Mikhail E. Itkis, and Robert C. Haddon*

Center for Nanoscale Science and Engineering, Departments of Chemistry and Chemical & Environmental Engineering, University of California, Riverside, California 92521-0403

Received April 24, 2003. Revised Manuscript Received July 31, 2003

Electric-arc produced as-prepared single-walled carbon nanotube (AP-SWNT) films have been purified by a selective oxidation process. The purification is monitored by near-infrared (NIR) spectroscopy, which gives a quantitative estimate of relative purities. This technique also gives an estimate of the change in relative amounts of SWNTs and amorphous carbon impurities after each purification step, thereby providing accurate and selective control over the oxidation process. Oxidation was carried out by reaction in flowing oxygen at different temperatures and for different durations of time; the purity was evaluated after each oxidation step and compared to the starting as-prepared film. The purities and amounts of SWNTs and carbonaceous impurities were monitored as a function of oxidation temperature and time. Optimization of the process allowed a 3-fold improvement in the AP-SWNT purity with almost quantitative retention of the SWNT portion of the sample. A purification efficiency is defined, which is expressed as the ratio of the fraction of SWNTs retained to the fraction of impurities retained in the sample after application of the purification process.

Introduction

Single-walled carbon nanotubes (SWNTs) have attracted considerable interest in recent years due to their unique one-dimensional structure and a range of fascinating properties.[1,2] Many interesting and useful applications have been suggested for carbon nanotubes such as fillers for high-strength composites,[3,4] gas sensors,[5,6] hydrogen storage media,[7] field emitters,[8−10] and nano-electronic devices.[11−13] Large quantities of pure SWNTs are required for many of these applications. Reasonable amounts of SWNTs can be obtained from the Ni−Y catalyzed arc-discharge process[14] but the products are always contaminated with impurities that include residual metal catalyst, amorphous carbon, and graphitic nanoparticles. Various techniques have been reported in the literature to purify SWNT samples such as microfiltration,[15,16] treatment with acids,[17−24] microwave heating,[25] and gas-phase oxidation.[26] However, despite the large number of reports on the purification of SWNTs, almost no information is available on the efficiencies of these processes, and the final purity and yield of the SWNTs after processing.

* Corresponding author. E-mail: haddon@ucr.edu.

(1) Dresselhaus, M. S.; Dresselhaus, G.; Avouris, P. *Carbon Nanotubes: Synthesis, Structure, Properties and Applications*; Springer-Verlag: Berlin, 2001; Vol. 80.
(2) Niyogi, S.; Hamon, M. A.; Hu, H.; Zhao, B.; Bhowmik, P.; Sen, R.; Itkis, M. E.; Haddon, R. C. *Acc. Chem. Res.* **2002**, *35*, 1105−1113.
(3) Calvert, P. *Nature* **1999**, *399*, 210−211.
(4) Andrews, R.; Jacques, D.; Rao, A. M.; Rantell, T.; Derbyshire, F.; Chen, Y.; Chen, J.; Haddon, R. C. *Appl. Phys. Lett.* **1999**, *75*, 1329−1331.
(5) Collins, P. G.; Bradley, K.; Ishigami, M.; Zettl, A. *Science* **2000**, *287*, 1801−1804.
(6) Adu, C. K. W.; Sumanasekera, G. U.; Pradhan, B. K.; Romero, H. E.; Eklund, P. C. *Chem. Phys. Lett.* **2001**, *337*, 31−35.
(7) Dillon, A. C.; Jones, K. M.; Bekkedahl, T. A.; Kiang, C. H.; Bethune, D. S.; Heben, M. J. *Nature* **1997**, *386*, 377−379.
(8) de Heer, W. A.; Chatelain, A.; Ugarte, D. *Science* **1995**, *270*, 1179−1180.
(9) Rao, A. M.; Jacques, D.; Haddon, R. C.; Zhu, W.; Bower, C.; Jin, S. *Appl. Phys. Lett.* **2000**, *76*, 3813−3815.
(10) Zhu, W.; Bower, C.; Zhou, O.; Kochanski, G.; Jin, S. *Appl. Phys. Lett.* **1999**, *75*, 873−875.
(11) Ouyang, M.; Huang, J.-L.; Lieber, C. M. *Acc. Chem. Res.* **2002**, *35*, 1018−1025.
(12) Avouris, P. *Acc. Chem. Res.* **2002**, *35*, 1026−1034.
(13) Satishkumar, B. C.; Thomas, P. J.; Govindaraj, A.; Rao, C. N. R. *Appl. Phys. Lett.* **2000**, *77*, 2530−2532.
(14) Journet, C.; Maser, W. K.; Bernier, P.; Loiseau, A.; Lamy de la Chappelle, M.; Lefrant, S.; Deniard, P.; Lee, R.; Fischer, J. E. *Nature* **1997**, *388*, 756−758.
(15) Bandow, S.; Rao, A. M.; Williams, K. A.; Thess, A.; Smalley, R. E.; Eklund, P. C. *J. Phys. Chem. B* **1997**, *101*, 8839−8842.
(16) Shelimov, K. B.; Esanaliev, R. O.; Rinzler, A. G.; Huffman, C. B.; Smalley, R. E. *Chem. Phys. Lett.* **1998**, *282*, 429−434.
(17) Rinzler, A. G.; Liu, J.; Dai, H.; Nilolaev, P.; Huffman, C. B.; Rodriguez-Macias, F. J.; Boul, P. J.; Lu, A. H.; Heymann, D.; Colbert, D. T.; Lee, R. S.; Fischer, J. E.; Rao, A. M.; Eklund, P. C.; Smalley, R. E. *Appl. Phys. A* **1998**, *67*, 29−37.
(18) Rao, C. N. R.; Govindaraj, A.; Sen, R.; Satishkumar, B. C. *Mater. Res. Innovat.* **1998**, *2*, 128−141.
(19) Dillon, A. C.; Gennet, T.; Jones, K. M.; Alleman, J. L.; Parilla, P. A.; Heben, M. J. *Adv. Mater.* **1999**, *11*, 1354−1358.
(20) Shi, Z.; Lian, Y.; Liao, F. H.; Zhou, X.; Gu, Z.; Zhang, Y.; Iijima, S. *Solid State Commun.* **1999**, *112*, 35−37.
(21) Chiang, I. W.; Brinson, B. E.; Smalley, R. E.; Margrave, J. L.; Hauge, R. H. *J. Phys. Chem. B* **2001**, *105*, 1157−1161.
(22) Chiang, I. W.; Brinson, B. E.; Huang, A. Y.; Willis, P. A.; Bronikowski, M. J.; Margrave, J. L.; Smalley, R. E.; Hauge, R. H. *J. Phys. Chem. B* **2001**, *105*, 8297−8301.
(23) Moon, J. M.; An, K. H.; Lee, Y. H.; Park, Y. S.; Bae, D. J.; Park, G. S. *J. Phys. Chem. B* **2001**, *105*, 5677−5681.
(24) Kajiura, H.; Tsutsui, S.; Huang, H.; Murakami, Y. *Chem. Phys. Lett.* **2002**, *364*, 586−592.
(25) Harutyunyan, A. R.; Pradhan, B. K.; Chang, J.; Chen, G.; Eklund, P. C. *J. Phys. Chem. B* **2002**, *106*, 8671−8675.
(26) Zimmerman, J. L.; Bradley, R. K.; Huffman, C. B.; Hauge, R. H.; Margrave, J. L. *Chem. Mater.* **2000**, *12*, 1361−1366.

10.1021/cm0342997 CCC: $25.00 © 2003 American Chemical Society
Published on Web 09/18/2003

Gas-phase oxidation (heating in air, oxygen, or other gases) is based on the idea of a selective oxidative etching process, wherein the carbonaceous impurities are oxidized at a faster rate than the SWNTs.[26] Nevertheless, the SWNTs can also be etched away during the oxidation, and precise control and calibration of the oxidation temperature and time duration are needed. Many different air oxidation temperatures and time durations have been reported and in many of these cases the yield of the final product is low, which implies that a large fraction of the SWNTs are consumed in the process.[20,24] It is therefore important to develop a purification in which the carbonaceous impurities are selectively oxidized while leaving the SWNTs intact. To achieve this, it is necessary to examine the evolution of a characteristic spectroscopic signal that allows differentiation of the SWNTs from the amorphous carbon impurities as the processing conditions are varied.

This raises the issue of quantifying SWNT purity. Microscopic techniques such as scanning electron microscopy (SEM) and transmission electron microscopy (TEM) have been used to evaluate SWNT purity but these techniques have inherent drawbacks due to the minute sample size and inhomogeneity of SWNT samples.[23,27] Near-infrared (NIR) spectroscopy has been established as an important tool for characterizing the electronic band structure of SWNTs.[28−32] All as-prepared (AP-) SWNT samples contain nanotubes with a range of diameters and chiralities, which lead to a mixture of semiconducting and metallic SWNTs. The NIR spectra of SWNTs exhibit peaks that arise due to transitions between the van Hove singularities in the electronic density of states of the SWNTs. A typical NIR transmittance spectrum of an arc-produced SWNT film is shown in Figure 1a. The spectrum shows three main peaks at 5500, 9800, and 13 800 cm^{-1} superimposed on a broad absorption band which shows a maximum at 37 000 cm^{-1} (not shown in the figure). The first two peaks are due to semiconducting SWNTs with $S_{11} = 2a\beta/d$ and $S_{22} = 4a\beta/d$, while the third peak is due to metallic SWNTs ($M_{11} = 6a\beta/d$), where a is the carbon−carbon bond length (nm), β is the transfer integral between pπ orbitals, and d is the SWNT diameter. These prominent features in the NIR spectral range can be used to analyze the SWNT type and diameter and the effect of doping.[28−31,33] The broad absorption band arises from π-plasmon excitation in both SWNTs and graphitic impurities.[34] If we consider the absorption band in the spectral region of one of the interband transitions (for example the S_{22} peak) for a standard SWNT sample, then the integrated area under this peak can be divided into three parts as shown in Figure 1b. AA(S) is the aerial absorption of the peak after baseline subtraction as shown in Figure 1c and is due to the interband transition in the SWNTs. The aerial absorption under the baseline has contributions from the π-plasmon of SWNTs (AA(N)) and carbonaceous impurities (AA(I)). AA(T) is the total aerial absorption under the peak without baseline subtraction and is a sum of AA(S), AA(N), and AA(I).

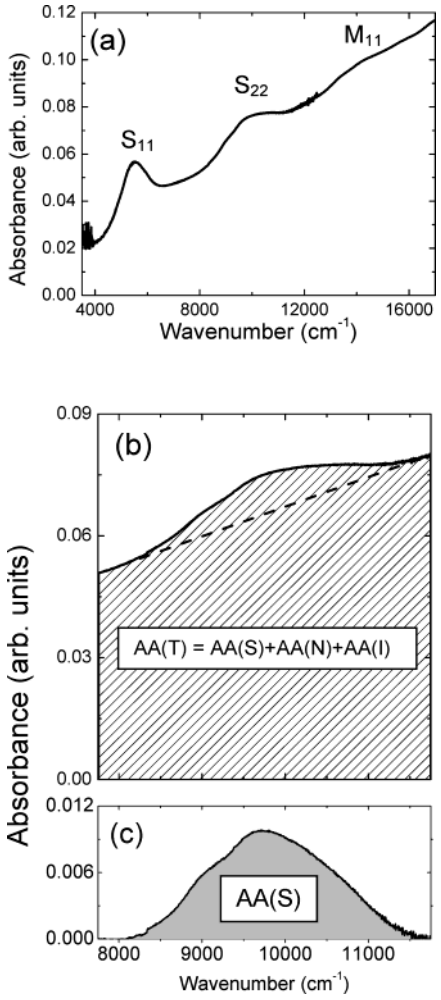

Figure 1. (a) NIR spectrum of a typical AP-SWNT film. S_{11} and S_{22} denote the first and second transition for semiconducting SWNTs and M_{11} denotes the first transition for metallic SWNTs. (b) Region of the spectrum from 7750 to 11 750 cm^{-1}, which includes the S_{22} peak. The shaded portion (AA(T)) is the total aerial absorption of the peak. (c) The S_{22} peak after baseline subtraction. The gray area (AA(S)) is the aerial absorption of the peak after baseline subtraction.

This allows the definition of a relative purity (RP) which is given by the expression

$$RP(X) = \{[AA(S, X)] \times [AA(T, X)]^{-1}\}/\{[AA(S, R)] \times [AA(T, R)]^{-1}\} \quad (1)$$

where AA(T) = AA(S) + AA(N) + AA(I), X is a SWNT sample of unknown purity, and R is a reference SWNT sample. It has been previously demonstrated that solution-phase NIR spectroscopy is a rapid and effective means of evaluating the purity of arc-produced SWNT samples.[35] In this study, the sample obtained from the

(27) Morishita, K.; Takarada, T. *J. Mater. Sci.* **1999**, *34*, 1169−1174.
(28) Chen, J.; Hamon, M. A.; Hu, H.; Chen, Y.; Rao, A. M.; Eklund, P. C.; Haddon, R. C. *Science* **1998**, *282*, 95−98.
(29) Kataura, H.; Kumazawa, Y.; Maniwa, Y.; Umezu, I.; Suzuki, S.; Ohtsuka, Y.; Achiba, Y. *Synth. Met.* **1999**, *103*, 2555−2558.
(30) Kazaoui, S.; Minami, N.; Jacquemin, R.; Kataura, H.; Achiba, Y. *Phys. Rev. B* **1999**, *60*, 13339−13342.
(31) Itkis, M. E.; Niyogi, S.; Meng, M.; Hamon, M.; Hu, H.; Haddon, R. C. *NanoLett.* **2002**, *2*, 155−159.
(32) Bachilo, S. M.; Strano, M. S.; Kittrell, C.; Hauge, R. H.; Smalley, R. E.; Weisman, R. B. *Science* **2002**, *298*, 2361−2366.
(33) Jost, O.; Gorbunov, A. A.; Pompe, W.; Pichler, T.; Friedlein, R.; Knupfer, M.; Reibold, M.; Bauer, H.-D.; Dunsch, L.; Golden, M. S.; Fink, J. *Appl. Phys. Lett.* **1999**, *75*, 2217−2219.
(34) Pichler, T.; Knupfer, M.; Golden, M. S.; Fink, J.; Rinzler, A.; Smalley, R. E. *Phys. Rev. Lett.* **1998**, *80*, 4729−4732.
(35) Itkis, M. E.; Perea, D.; Niyogi, S.; Rickard, S.; Hamon, M.; Hu, H.; Zhao, B.; Haddon, R. C. *Nano Lett.* **2003**, *3*, 309−314.

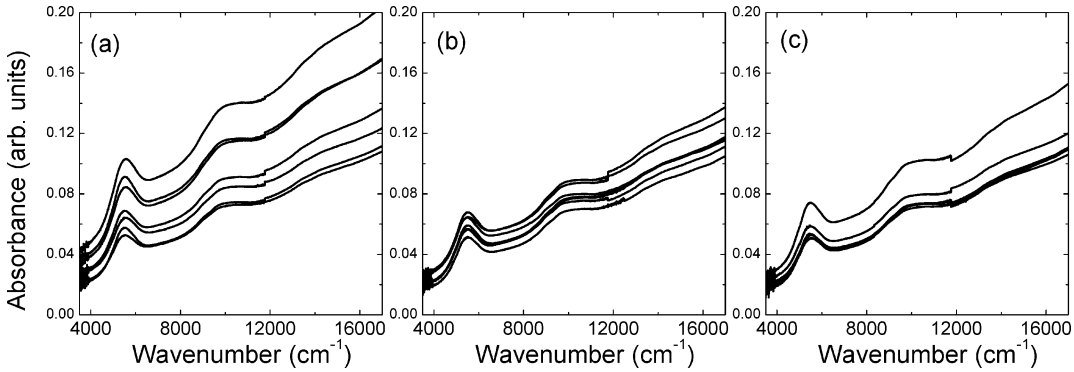

Figure 2. NIR spectra of AP-SWNT films from 3 different batches, each containing data from 7 different films: (a) batch 1, (b) batch 2, and (c) batch 3.

web region of the arc-discharge process was used as the reference ($R2$).[35]

In the present paper we report a systematic study on the purification of AP-SWNT films by heating in flowing oxygen gas and we make use of NIR spectroscopy to monitor this process. It is important to note that the data presented refer to the oxygenation reaction undergone by the AP-SWNTs in the presence of the Ni−Y catalyst used in their manufacture. The metal nanoparticles present in the sample are known to catalyze the oxidation of SWNTs.[21,25]

The relative purity was calculated from the NIR spectra according to our previous report.[35] The S_{22} band in the spectral region 7750−11 750 cm^{-1} was selected for the purity analysis, as this band is least influenced by doping effects. Because we are examining the effect of the oxidation temperature and time on the purity of SWNT films, we have used the starting AP-SWNT film as the reference in each case. The variation in the AA(S) value is monitored as an indicator of the amount of SWNTs remaining after oxidation, and the change in AA(T) value is used as an indicator for the carbonaceous impurities. The efficiency of the process can be followed by monitoring the behavior of the AA(S) and AA(T) values. A small decrease in AA(S) value and a large decrease in AA(T) value on oxidation would indicate that a large percentage of the carbonaceous impurities have been etched away while most of the SWNTs remain intact. This will also be reflected in the relative purity values, which can be calculated from the following equation:

$$RP(OX) = \{AA(S, OX)/AA(T, OX)\}/\{AA(S, AP)/AA(T, AP)\} \quad (2)$$

where OX refers to the oxygen-reacted SWNT film and AP refers to the as-prepared (starting) SWNT film.

By monitoring the AA(S), AA(T), and RP values as a function of oxidation temperature and time it is possible to quantitatively investigate the oxidative etching of the film constituents.

Experimental Section

Materials. SWNTs were made by the electric arc process using Ni and Y catalysts and were used as received from Carbon Solutions, Inc. The relative purity of the AP-SWNT used in this study was determined to be 35% by NIR spectroscopy.[35]

AP-SWNT soot (10 g) was mechanically homogenized, and 50 mg of this homogenized soot was dispersed in dimethylformamide (DMF, 250 mL) by ultrasonicating for 30 min. During this process, a homogeneous slurry of the AP-SWNT soot was obtained. The slurry (10 mL) was loaded into a volatilizer and sprayed onto the glass slides using argon. The glass slides were maintained at 160 °C during the spraying process. The film thickness was monitored visually, and if nonuniformity was evident the films were rejected; the films were allowed to cool in air and characterized by NIR spectroscopy.

Oxygen Treatment of the SWNT Films. The AP-SWNT films were loaded into a glass tube fitted inside a tube furnace. Argon gas was flowed through the tube and the temperature of the furnace was ramped up to the desired set point. The films were soaked at this temperature overnight in flowing argon to stabilize the temperature of the film. The temperature was measured by attaching the probe of a thermocouple onto the glass tube, very close to the SWNT film. This provided a reproducible and accurate estimate of the temperature of the film. Once the temperature had stabilized to a level of ±2 °C of the set point, the argon flow was switched to pure oxygen. Reaction under the oxygen flow was carried out for different time durations and the films were then allowed to cool under pure argon flow. In the present experiments we used three different set point temperatures of 265, 292, and 315 °C for up to 6 h oxidation time. Lower oxidation temperatures of 210, 235, and 245 °C were also examined for longer duration (12 h).

NIR Spectroscopy. NIR spectra of the films, before and after oxidation, were recorded on a CARY 500 Scan UV−Vis−NIR spectrophotometer. The scan range was from 3500 to 17 000 cm^{-1}. Double beam mode was used and a spectrum was first collected using two blank glass slides. To collect the spectrum of the sample, one of the blank slides was replaced with a slide containing the SWNT film, and the spectrum was re-collected under the same conditions. The film spectrum was then automatically corrected for the blank glass slide.

Results and Discussion

NIR transmission spectroscopy of SWNT films has been reported in the literature.[29,31,33,36] However, the reproducible preparation of uniform films is difficult. We have addressed this issue by preparing a number of films from the same AP-SWNT material and carrying out NIR spectroscopic analyses on these films before the oxidation experiments. Figure 2 shows the NIR spectra of 21 AP-SWNT films from three different batches (seven films from each batch). A statistical analysis of the three batches is given in Table 1. The mean AA(S) value for batch 1 is 22.0 with a standard deviation of 4.8. The standard deviation and the minimum and

(36) Hennrich, F.; Lebedkin, S.; Malik, S.; Tracy, J.; Barczewski, M.; Rosner, H.; Kappes, M. *Phys. Chem. Chem. Phys.* **2002**, *4*, 2273−2277.

Table 1. Statistical Analysis of the NIR Data for Different Batches of AP-SWNT Films

	batch 1	batch 2	batch 3	batches1 + 2 + 3
mean AA(S)	22.0	18.1	19.0	19.7
s.d.	4.8	1.3	2.6	3.5
min. AA(S)	16.1	16.5	16.7	16.1
max. AA(S)	29.4	20.3	24.5	29.4
mean AA(T)	361	288	283	311
s.d.	92	25	40	67
min. AA(T)	265	252	259	252
max. AA(T)	509	324	370	509
mean AA(S)/AA(T)	0.0615	0.0629	0.0673	0.0639
s.d.	0.0033	0.0036	0.0023	0.0039
min. AA(S)/AA(T)	0.0579	0.0574	0.0643	0.0574
max. AA(S)/AA(T)	0.0683	0.0668	0.0709	0.0709

maximum values shown in Table 1 reflect a large variability in the AA(S) values for the films prepared in batch 1, which is also evident from the NIR spectra shown in Figure 2a. The AA(T) values for batch 1 show a large range, from 265 to 509, with a mean value of 361, and standard deviation of 92. Despite the large variability in the AA(S) and AA(T) values for batch 1, the ratio of AA(S) and AA(T) values shows much less scatter about the mean. The mean AA(S)/AA(T) value for batch 1 is 0.0615 and the standard deviation is 0.0033. This result indicates that even with a variability in the AA(S) and AA(T) values, the AA(S)/AA(T) ratio that is used to calculate the relative purity is much more reliable. This means that the purity values of the AP-SWNT films are quite consistent within batch 1. For batch 2, the AA(S) value has a mean of 18.1 and a standard deviation of 1.3 and the AA(T) value has a mean of 288 and a standard deviation of 25. This shows that batch 2 has much less scatter in the AA(S) and AA(T) values when compared to batch 1. However, the AA(S)/AA(T) ratio for batch 2 has a standard deviation of 0.0036 which is very similar to the scatter for batch 1. This shows that despite the differences in variability in the AA(S) and AA(T) values, the AA(S)/AA(T) values for the two batches have similar scatter. The scatter in AA(S) and AA(T) values for batch 3 is between those for batch 1 and 2 (Figure 2 and Table 1). However, batch 3 shows much less scatter in the AA(S)/AA(T) values (standard deviation of 0.0023). There are two important factors that arise from the statistical analysis. First, even though there is a variation in the mean AA(S) and AA(T) values for the three batches, the mean AA(S)/AA(T) values have much less scatter. Because the AA(S)/AA(T) value is a measure of the purity of the samples, the low variability in this value confirms that the purity evaluations of the AP-SWNT films are consistent within a batch. Second, the mean AA(S)/AA(T) values are very similar for the three different batches, therefore the purities of the films are also consistent from batch to batch. A statistical analysis of all the 21 films taken together is given in the last column of Table 1. This column shows that the mean and standard deviation for AA(S)/AA(T) for all three batches taken together are consistent with the values for the individual batches. To ensure consistent results, all our oxidation studies were carried out on films which had AA(S) values between 16 and 30, AA(T) values between 250 and 510, and AA(S)/AA(T) values between 0.057 and 0.071. These values were selected as the optimum compromise between instrumental sensitivity and light scattering in the films that is evident at high SWNT loadings.

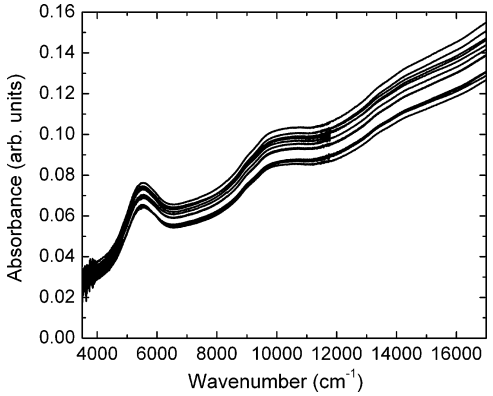

Figure 3. NIR spectra from twelve different positions of the same AP-SWNT film.

Having established that the 21 different AP-SWNT films are internally consistent in terms of the purity evaluation, we then examined the variability of the SWNT purity within a film. Inhomogeneity during the spraying process may lead to a nonuniform film thickness and variability in the NIR results. To check these factors we obtained NIR spectra from different positions on a typical film. NIR spectra from 12 different positions of an AP-SWNT film are shown in Figure 3. These 12 positions cover the entire film (Figure 4a). From Figure 3 it is clear that the NIR spectra from different positions on the film are very similar, nevertheless there is some variation in the AA(S) and AA(T) values. Figure 4b and c shows bar graphs of the AA(S) and AA(T) values from the 12 different positions indicated in Figure 4a. A careful examination of Figure 4b and c reveals that the AA(S) and AA(T) values tend to increase from positions A1, B1, C1 to A4, B4, C4 (left to right on the film in Figure 4a). This may be due to a variation in the thickness of the film. However, the variation in the AA(S)/AA(T) values as shown in Figure 4d do not show any trend and are quite random. The mean AA(S)/AA(T) value is 0.0589 with a standard deviation of 0.0022. Therefore the AA(S)/AA(T) values from different positions on the film do not exhibit a large variation. For all our subsequent studies we have recorded NIR spectra from three different positions on each film to allow for the effect of inhomogeneity in the film.

The reactions with flowing oxygen were carried out at three different temperatures: 265, 292, and 315 °C. The films were soaked at the desired temperature overnight under argon flow before beginning the oxygen flow. Therefore, we first examined the effect of annealing in argon for 12 h on the film purity. Figure 5a and b shows NIR spectra for an AP-SWNT film before and after annealing in argon flow for 12 h at 315 °C. There is little change in the NIR spectrum on annealing in argon. Purity calculations reveal that the relative purity (RP) of the argon-annealed film was 1.2 when compared to the AP-SWNT film. This marginal increase in the purity could be due to the removal of volatile impurities from the film. Because we carry out 12-h argon anneal at the same temperature for all the films prior to the oxidation step, the argon annealing effect will be same for all the films and will not be reflected in the interpretation of the oxidation results.

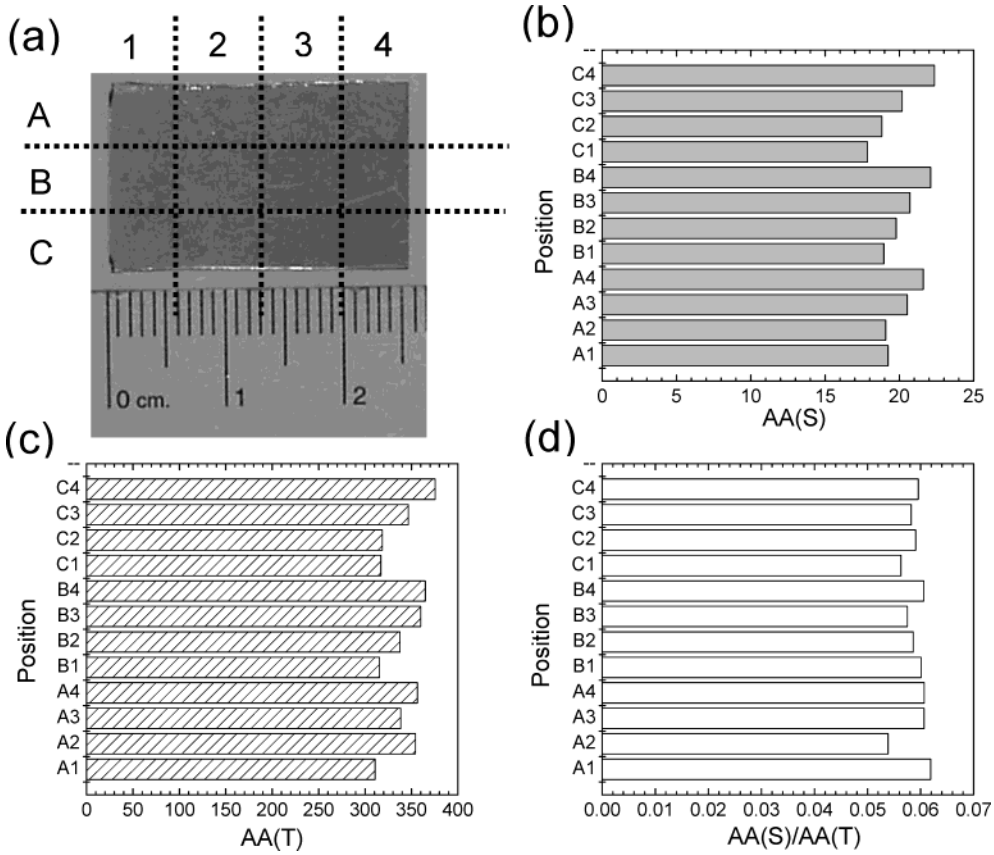

Figure 4. (a) Photograph of the film showing the division of the SWNT film into regions for recording the NIR spectra (see Figure 3). Bar graphs showing (b) aerial absorption under the peak after baseline subtraction (AA(S)), (c) total aerial absorption under the peak (AA(T)), and (d) the AA(S)/AA(T) ratio obtained by analyzing NIR spectra from different positions on the film.

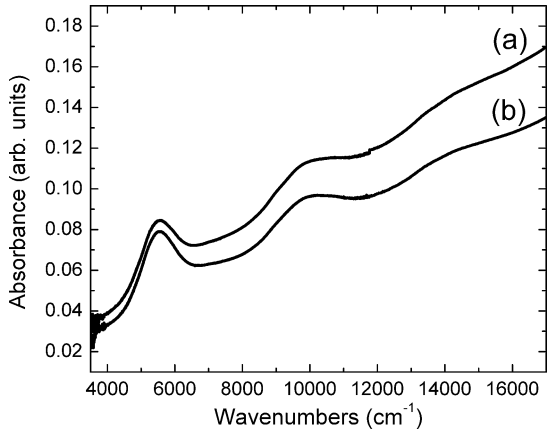

Figure 5. NIR spectra of an AP-SWNT film (a) before and (b) after annealing in argon atmosphere at 315 °C for 12 h.

Figure 6a and b shows NIR spectra for an AP-SWNT film before and after reaction with oxygen flow at 292 °C for 4 h. Comparing Figure 6 panels a and b it is clear that the NIR spectrum of the oxygen-reacted film has an absorption background of much lower intensity and a smaller slope when compared to the AP-SWNT film. AA(T), the aerial absorption under the S_{22} peak together with the broad absorption background, drops from 278.6 to 66.5 after oxidation. These features are represented as AA(T, AP) and AA(T, OX) in Figure 6c and d. The aerial absorption under the S_{22} peak after subtracting the background is 17.6 for AP-SWNT film (AA(S, AP)) and 12.8 for the oxygen-reacted film (AA(S, OX)), as shown in Figure 6e and f, respectively. Therefore the aerial absorption of the S_{22} peak, AA(S), decreases by only 27% on reacting the AP-SWNT film with flowing oxygen for 4 h at 292 °C, whereas the same treatment decreases the AA(T) value by 76%. This large decrease in the AA(T) value can be attributed to a decrease in the amount of amorphous carbon impurities. Thus, the relative purity (RP) of the film reacted with flowing oxygen at 292 °C for 4 h is 3.0 with respect to the AP-SWNT film (eq 2). The increase in the relative purity indicates that a large percentage of the carbonaceous impurities have been removed by the oxidative etching process, whereas most of the SWNTs survived the treatment.

This type of oxidative etching is very sensitive to the oxidation temperature and time. We have carried out a systematic study of the selective oxidative etching process as a function of the oxidation temperature and time durations. The results are summarized in Figure 7. Figure 7a shows [AA(S, OX)/AA(S, AP)] × 100 values as a function of oxidation time for different temperatures. Three AA(S) values were calculated from the NIR spectra from three different positions on the film before and after each oxidation step. Therefore nine [AA(S, OX)/AA(S, AP)] × 100 values can be obtained from all possible combinations of the three AA(S, OX) and three AA(S, AP) values for a particular oxidation temperature and time. The mean value is plotted in Figure 7a and the standard deviation is shown as error bars in the graph. The mean [AA(T, OX)/AA(T, AP)] × 100 and RP values and their error bars plotted in Figure 7 panels b and c were calculated in the same manner.

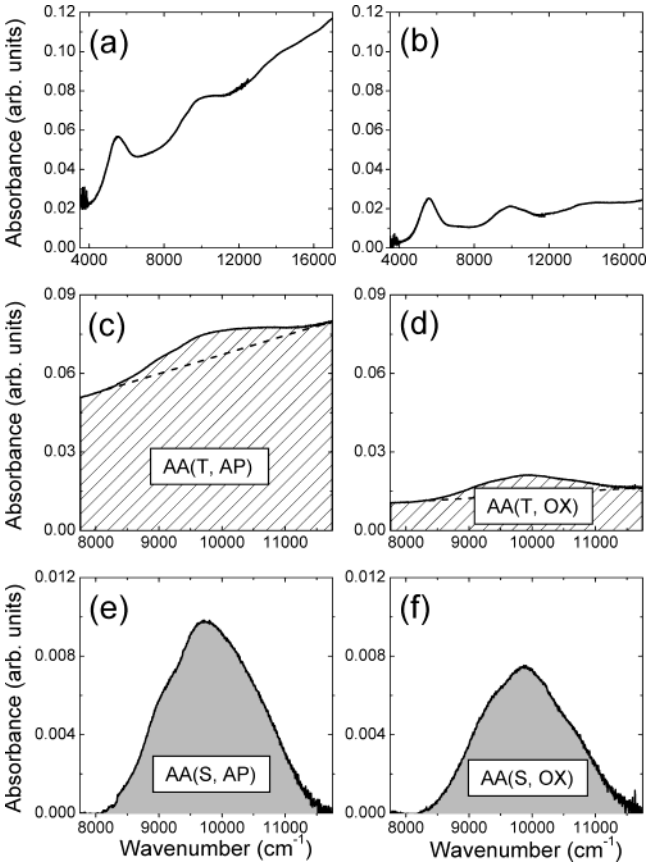

Figure 6. (a) NIR spectrum of an AP-SWNT film and (b) NIR spectrum of the same film after reaction with flowing oxygen atmosphere at 292 °C for 4 h. (c) Spectrum of the AP-SWNT film in the region 7750−11 750 cm^{-1} and (d) spectrum of the oxygen-reacted film in the region 7750−11 750 cm^{-1}. The shaded portions, AA(T, AP) and AA(T, OX), represent the total aerial absorption of the as-prepared and the oxygen-reacted films, respectively. The dashed line shows the baseline chosen for the background absorption correction. (e) and (f) S_{22} peak after baseline subtraction for the as-prepared and the oxygen-reacted films, respectively. The gray portions, AA(S, AP) and AA(S, OX), represent the aerial absorption under the peak after baseline subtraction for as-prepared and the oxygen-reacted films, respectively.

The [AA(S, OX)/AA(S, AP)] × 100 represents the percentage of SWNTs remaining after the oxidation step. Figure 7a shows that for reaction with flowing oxygen at 265 °C, the [AA(S, OX)/AA(S, AP)] × 100 values (black squares) decrease at a very slow rate with increasing oxidation time. This suggests that at this temperature the SWNTs are fairly stable to oxygen even in the presence of the metal catalyst. The [AA(T, OX)/AA(T, AP)] × 100 values at 265 °C (black squares in Figure 7b) decrease at a fast rate after 1−2 h oxidation but decrease more slowly after 3 h. The relative purity (RP) shows a steady increase with oxidation time at this temperature (black squares in Figure 7c). A similar trend is observed for oxidation temperature of 292 °C (black circles in Figure 7). The [AA(S, OX)/AA(S, AP)] × 100 values decrease slowly with oxidation time, but the decrease in this case is larger than that for the 265 °C case. This means that the higher oxidation temperature of 292 °C etches away SWNTs at a faster rate when compared to that at 265 °C. The [AA(T, OX)/AA(T, AP)] × 100 values also show a faster decreasing rate than for the 265 °C case. Thus, both the SWNTs and amorphous carbon are etched away at slightly higher rates at 292 °C than at 265 °C. The RP values show a sharp increase in the initial time periods (1 to 4 h) and then level off, indicating that most of the amorphous carbon impurities have burned away and that further oxidation (beyond 6 h) only serves to destroy the SWNTs. This effect is more pronounced at the higher oxidation temperature of 315 °C (represented by black triangles in Figure 7). At this temperature both the [AA(S, OX)/AA(S, AP)] × 100 and [AA(T, OX)/AA(T, AP)] × 100 values decrease at a much faster rate, indicating that both amorphous carbon and SWNTs are burned away at an appreciable rate. However, the RP values increase for the first 2 h indicating the etching rate of SWNTs is lower than that for amorphous carbon. After 2 h oxidation, most of the amorphous carbon has been etched away (80% decrease in the AA(T, OX)/AA(T, AP) value) and further annealing only leads to the destruction of SWNTs. Thus, at 315 °C the RP values decrease for oxidation times beyond 2 h.

We also define an efficiency (PE) for the purification process; PE is obtained by multiplying the relative purity (RP) value with the AA(S, OX)/AA(S, AP) ratio for each purification step. In other words, the RP value is multiplied by the amount of SWNTs surviving after each oxidation step. PE is useful because the purity is not a sufficient measure with which to judge a purification process − a large decrease in the amount of SWNTs means that the purification process is not useful even though the RP may be high. This point is illustrated by considering the 4-h oxidation at 265 and 315 °C. Figure 7c shows that the relative purities for both these processing conditions are almost same, but from Figure 7a it is obvious that the amount of SWNTs lost after 4 h oxidation at 315 °C is much larger than that at 265 °C. Thus, the efficiency of purification at 315 °C is lower than at 265 °C, and this is clear from Figure 7d, where PE (RPx[AA(S, OX)/AA(S, AP)]) is plotted with respect to oxidation time.

We also examined the effect of low-temperature oxygen reaction with the SWNTs for a 12-h duration. Oxidation at 210, 235, and 245 °C for 12 h does not show much decrease in the AA(S) values as represented by the cluster of points in the upper right-hand corner of Figure 7a. This means that at these temperatures, oxidation for 12 h does not burn significant amounts of the SWNTs. But the AA(T) values shows a decreasing trend for all the three cases and the percentage decrease increases with increasing temperature. This is represented by the set of data points at the right side of Figure 7b (open square, open circle, and open triangle). For 210 °C oxidation for 12 h, the AA(T) value decreases by only 20%, which means that at this temperature neither SWNTs nor amorphous carbon impurities are oxidized by a significant amount. This is reflected by the RP value (Figure 7c, open square) which is just 1.2 with respect to the AP sample. Oxidation at 235 °C for 12 h shows no decrease in AA(S) but a 40% decrease in AA(T) value (open circles in Figure 7a and b), hence the purification is quite efficient. This is reflected in the higher RP value and higher purification factor. Oxidation at 245 °C for 12 h shows the best results as there is no decrease in AA(S) value whereas the AA(T) value decreases by about 55% (open triangles in Figure 7a and

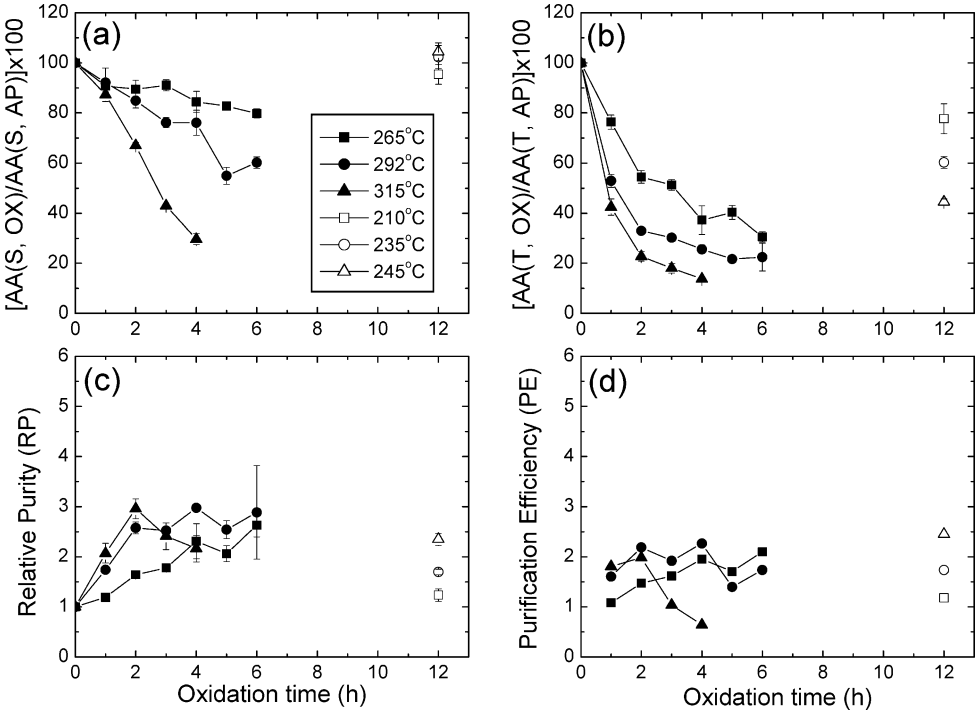

Figure 7. (a) Aerial absorption of the S_{22} peak after baseline subtraction for the oxygen-reacted SWNT film (AA(S, OX)) divided by the aerial absorption of the S_{22} peak for the corresponding as-prepared film (AA(S, AP)) as a function of oxidation time for different oxidation temperatures. The ordinate is a measure of the percentage of SWNTs remaining after each oxidation step. (b) Total aerial absorption under the peak for the oxygen-reacted film (AA(T, OX)) divided by the total aerial absorption of the corresponding as-prepared film (AA(T, AP)) as a function of oxidation time for different oxidation temperatures. The ordinate is a measure of the percentage of carbonaceous material (amorphous carbon impurities and SWNTs) remaining after each oxidation step, but is used as an indicator for the amorphous carbon impurities. (c) Relative purities (RP), where RP = {AA(S, OX)/AA(T, OX)}/{AA(S, AP)/AA(T, AP)}, as a function of oxidation time for different oxidation temperatures. (d) Purification efficiency factor (PE), where PE = RPx[AA(S, OX)/AA(S, AP)], as a function of oxidation time for different oxidation temperatures.

b). The relative purity (RP) is reasonably high with value of 2.35 and the purification efficiency factor has the highest value obtained so far.

Thus it is clear that NIR spectroscopy provides a convenient tool to monitor the progress of SWNT purification, and has allowed the optimization of the parameters involved in the thermal oxidative purification of SWNTs. Furthermore this approach to process optimization will have wide application in the study of other methods of SWNT purification.

Conclusions

We have shown that the oxidative etching of SWNTs and amorphous carbon impurities can be monitored precisely by calculating the AA(S), AA(T), and RP values from the NIR spectra. It is therefore possible to selectively burn away the amorphous carbon impurities while retaining most of the SWNTs. We expect that the application of the methods discussed above will allow the rapid optimization of SWNT purification procedures. Our studies have been carried out on SWNT films because the high surface area of the films exposes most of the material to the oxygen environment and consistent results may be obtained. However, for practical applications the technique must be scaled to bulk SWNTs samples. Gas permeability and packing density of the bulk material may be issues for bulk purification. Nevertheless, NIR spectroscopy in conjunction with the techniques described in this paper can be used to precisely monitor the process and thereby achieve high yield purification of SWNTs by selective oxidative etching of the carbonaceous impurities.

Acknowledgment. This work was supported by the MRSEC Program of the National Science Foundation under award DMR-9809686 and by DOD/DARPA/DMEA under award DMEA90-02-2-0216. Carbon Solutions, Inc. acknowledges NSF SBIR Phase I and II awards DMI-0110221 from the Division for Design, Manufacture and Industrial Innovation.

CM0342997